Journal of Advanced Ceramics
2014, 3(1): 76–82
DOI: 10.1007/s40145-014-0096-y

ISSN 2226-4108
CN 10-1154/TQ

Research Article

Effects of core/shell volumetric ratio on the dielectric-temperature behavior of $BaTiO_3$

Sang-Chae JEON[a], Byung-Kwon YOON[b], Kwan-Hyeong KIM[b], Suk-Joong L. KANG[a,*]

[a]*Materials Interface Laboratory*, *Department of Materials Science and Engineering*, *Korea Advanced Institute of Science and Technology*, *291 Daehak-ro*, *Yuseong-gu Daejeon 305-701*, *Korea*
[b]*LCR Division*, *Samsung Electro-Mechanics*, *Suwon 443-743*, *Korea*

Received: January 14, 2014; Accepted: January 27, 2014

Abstract: Two sets of (Mg,Y)-doped $BaTiO_3$ samples were prepared to investigate the effects of the core/shell volumetric ratio on the dielectric-temperature behavior of $BaTiO_3$: one set with samples of the same grain size but different core sizes and the other with samples of the same core size but different shell thicknesses. The microstructural variation of the samples was characterized and their dielectric properties were measured. For both sets of samples, the temperature stability of the dielectric properties was generally improved with a reduction of the volumetric shell ratio regardless of the grain and core sizes. There existed, however, a limit of the reduction; for the studied range, shell thickness of one third of the core radius appeared to be an optimum thickness for the given amounts of dopants. It was concluded that the volumetric shell ratio should be optimized so as not to exceed a specific limit, for our case two thirds of the grain volume, to secure temperature stability of the dielectric properties of $BaTiO_3$.

Keywords: barium titanate; core/shell structure; dielectric properties; temperature stability

1 Introduction

For multilayer ceramic capacitor (MLCC) applications, the dielectric properties of pure $BaTiO_3$ are modified to improve their temperature stability by adding solute elements. The addition of solute elements often results in the formation of an inhomogeneous microstructure during sintering that is typified by a core/shell structure [1–7]. A core/shell grain is a dual-phase grain that consists of a core phase at the center and a shell phase around the core. The shell phase is clearly distinguished from the core region by both its morphology (rare ferroelectric domains) and chemical composition (high concentration of additives). When a core/shell structure forms, the dielectric-temperature behavior of the sample is typically improved, showing insensitive variation of the dielectric properties in a wide temperature range while also satisfying industrial standards [8–10]. Because of its positive effect on dielectric behavior, the core/shell structure of $BaTiO_3$ has won attention from many researchers [2–6]. The improvement of the temperature-dependent behavior has been attributed to the contribution of the shell phase, which shows an appreciable displacement of the maximum dielectric constant down below room

* Corresponding author.
E-mail: sjkang@kaist.ac.kr

temperature with a broadened transition peak, so-called diffuse phase transition (DPT) behavior, similar to that of relaxor materials [11–14].

One of the important issues in the study of core/shell structure in both academic and industrial settings is the optimization of the system and microstructure to obtain desired dielectric-temperature characteristics. The effects of various kinds and amounts of additives have been studied [2,4,5,9,10,15–22], including in particular those of rare earth elements with intermediate ionic radii (Dy, Ho, Y and Er) [9,10,19–23]. In the case of rare earth doping, high insulation resistance can be maintained for a long time, which enables the realization of thinner dielectric layers and extended life time in the use of MLCCs [24].

The effects of processing parameters, such as ball milling time [6,25,26], thermal cycle [10] and sintering atmosphere [27], on the microstructure and dielectric properties of $BaTiO_3$ systems have also been investigated in relation to the variation of the core/shell volumetric ratio. Wang *et al*. [26] reported that in a (Mg,Y)-doped $BaTiO_3$ system, the shell thickness increases with a reduction of core size and the dielectric-temperature behavior is deteriorated as the ball milling time is increased. The shell thickening is attributed to a result of solid state diffusion of dopants in the shell. With the thickening of shell, however, the dopant concentration in the shell changes considerably. It is, therefore, difficult to differentiate the effects of the two parameters, the thickness and composition of the shell, on dielectric-temperature properties. Yasukawa *et al*. [25] observed a similar variation of dielectric-temperature properties with increased ball milling time. In their case, however, as the ball milling time increases, the chemistry in the shell as well as grain size vary considerably. Tian *et al.* [10] and McCauley *et al.* [27] observed a reduction of shell thickness by two-step sintering and thickening of the shell with a reduction of the oxygen partial pressure (p_{O_2}) during sintering. In both cases, also, the variation of shell thickness is accompanied by a considerable change in the dopant concentration in the shell.

The aim of this study is to clarify the effects of the volumetric ratio of the ferroelectric core and paraelectric shell on the dielectric-temperature behavior while minimizing other effects, such as chemical composition and grain size. Two sets of (Mg,Y)-doped $BaTiO_3$ samples with core/shell grains were prepared: one set with a constant grain size but different core/shell fractions and the other set with a constant core size but different shell thicknesses. The effects of both grain size and chemical composition were able to be minimized in the first set by controlling the chemistry of the starting material and changing the sintering time. The effect of shell thickness without having a core size effect was examined in the second set. Measurement of the dielectric properties of the samples shed light on the direction for optimizing the core/shell structure to attain temperature stability of dielectric properties.

2 Experimental procedure

Two sets of samples were prepared by the conventional ceramic processing technique from commercial powders. For the first set of experiments, to examine the effect of core size with the same grain size, samples were prepared from commercial $BaTiO_3$ powders of three different sizes, 0.6 μm① (99.6% purity, Fuji Titanium, Kanagawa, Japan), 0.3 μm (99.99% purity, Kyorix Co., Japan) and 0.1 μm (99.99% purity, Toda Kogyo Corp., Hiroshima, Japan) with addition of Y_2O_3 (99.9% purity, Kojundo Chemical Laboratory Co., Ltd., Japan), MgO (99.9% purity, Ube Material Industries, Ltd., Japan) and SiO_2 (99.85% purity, Wako Pure Chemical Industries, Ltd., Japan). The additives were common dopants of commercial $BaTiO_3$-based MLCCs with a core/shell structure. To prepare samples with shells having the same chemical composition, different amounts of dopants were added to the $BaTiO_3$ powders: $4Y_2O_3$–$4MgO$–$2SiO_2$ (mol%) to 0.1 μm $BaTiO_3$ powders (designated as 0.1BT), $3Y_2O_3$–$3MgO$–$2SiO_2$ to 0.3 μm $BaTiO_3$ powders (0.3BT) and $2Y_2O_3$–$2MgO$–$2SiO_2$ to 0.6 μm $BaTiO_3$ powders (0.6BT). The specific amounts of dopants for different samples were empirically determined after a preliminary experiment for finding proper compositions to keep the chemistry in the shell to be similar. The powder mixture was ball-milled for 24 h in a polypropylene bottle using ZrO_2 balls and a high-purity ethanol medium. The ball-milled powders were dried and passed through a 125 μm sieve. The granulated powders were lightly pressed in a steel die to make pellets of 9 mm in diameter and 3 mm in thickness. The pellets were then cold isostatically

①Although the size noted by the producer was 1.4 μm, the 3-dimensional particle size measured from SEM images was 0.56 μm. We denoted the particle size as the measured size.

pressed at 200 MPa and sintered in wet H_2 for various sintering time (15 min–4 h) at different temperatures (1300–1350 ℃). The sintered samples were oxidized at 1050 ℃ for 10 h in flowing air.

For the second set, samples with the same core size but different shell thicknesses were prepared from the Fuji Titanium $BaTiO_3$ powders of 0.6 μm in size with addition of 4 mol% of Y_2O_3, 4 mol% of MgO and 2 mol% of SiO_2. The proportioned powder mixtures were ball-milled, dried, sieved and pelletized using the same procedure as applied for the samples of the first set. The pellets were cold isostatically pressed at 200 MPa and then sintered at 1350 ℃ in wet H_2 for various periods of time from 0.5 h

The absolute bulk densities of all the sintered samples were measured by the Archimedes method. The microstructures of the samples were observed using a Phillips XL30 scanning electron microscope (SEM) (Phillips, Eindhoven, the Netherlands) after sectioning, polishing and chemical etching in a 95H_2O–4HCl–1HF (vol%) solution. Assuming that both grains and cores have spherical shape, the volumetric percentages of the cores (V_{core}) and their diameters (D_{core}) were estimated from the measured radii of more than 50 core/shell grains. The microstructures were also observed under a transmission electron microscope (TEM, JEOL Ltd., Tokyo, Japan) operated at 200 kV. The TEM samples were prepared by the conventional TEM sample preparation technique. The chemical composition of the samples was measured by energy-dispersive X-ray spectroscopy (TEM/EDS) line scanning in the TEM. For measurement of dielectric properties, the oxidized samples were coated with an Ag paste on both sides of the disk samples. The capacitance and dissipation factor were measured using an Agilent 4284A precision LCR meter at temperature ranging from –55 ℃ to 150 ℃ with a heating/cooling rate of 0.8 ℃/min at 1 kHz under 1 V_{rms}.

3 Results and discussion

Figure 1 presents schematic microstructures of the two different sets of samples. In the first set (Fig. 1(a)), the grains contain cores of different sizes but with a similar grain size. In the second set (Fig. 1(b)), the core/shell grains have cores of an identical size but with different shell thicknesses. As the shell forms and grows via a dissolution/precipitation process [2,5,7], it is possible to prepare samples with schematic microstructures as presented in Fig. 1 by using $BaTiO_3$ powders of different sizes for the first set and by varying the sintering time for the second set, respectively.

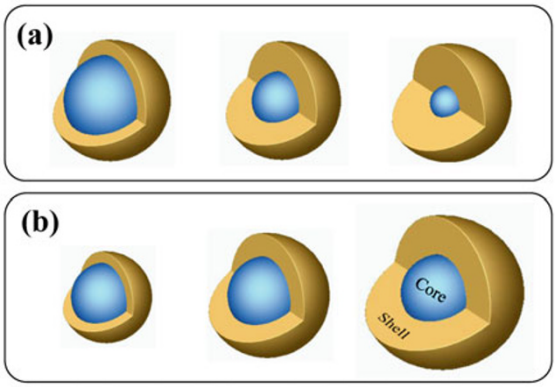

Fig. 1 Schematic illustrations showing the core/shell structures (a) in the first set with different core sizes and a similar grain size and (b) in the second set with a similar core size but different shell thicknesses.

Figure 2 shows SEM micrographs of the samples in the first set with different core sizes: 0.6 μm (Fig. 2(a), designated as 0.6BT), 0.3 μm (Fig. 2(b), 0.3BT) and 0.1 μm (Fig. 2(c), 0.1BT). The bulk densities do not vary substantially among samples, falling between 5.6 g/cm^3 and 5.8 g/cm^3. A core/shell structure of biphasic grains is clearly revealed in the SEM micrographs. The average 2-dimensional core sizes are measured to be 0.61 μm for 0.6BT, 0.32 μm for 0.3BT and 0.17 μm for 0.1BT, respectively. On the other hand, the measured average sizes of core/shell grains in the samples are not substantially different: 0.65 μm, 0.59 μm and 0.58 μm for 0.6BT, 0.3BT and 0.1BT, respectively. We can thus examine the core size effect in the absence of possible effect of grain size on dielectric properties. Figure 3 presents TEM micrographs of core/shell grains of the 0.3BT and 0.1BT samples (Figs. 3(a) and 3(b), respectively) and the measured concentration variations across the cores (Figs. 3(c) and 3(d), respectively). The TEM/EDS line scanning shows that the concentration of Y in the shell is around 2.5 at% while that in the core is close to nil in both samples. Note that the concentrations in the shells of different samples are similar. These microstructural and chemical characteristics allow us to examine the effect of core size while excluding the effect of grain size and the chemical composition of the shell.

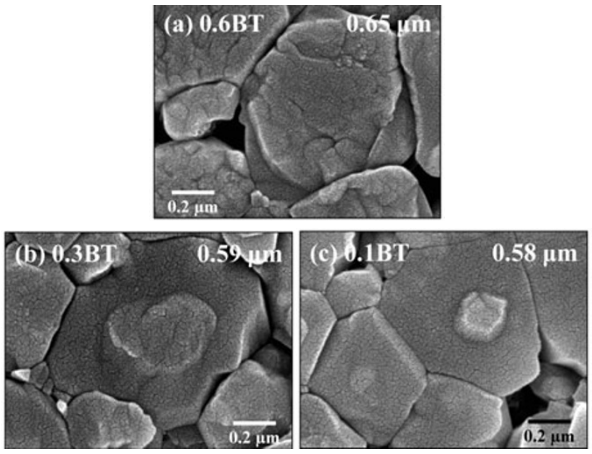

Fig. 2 SEM micrographs of (a) 0.6BT, (b) 0.3BT and (c) 0.1BT in the first set. The numbers in the micrographs are the measured average grain sizes.

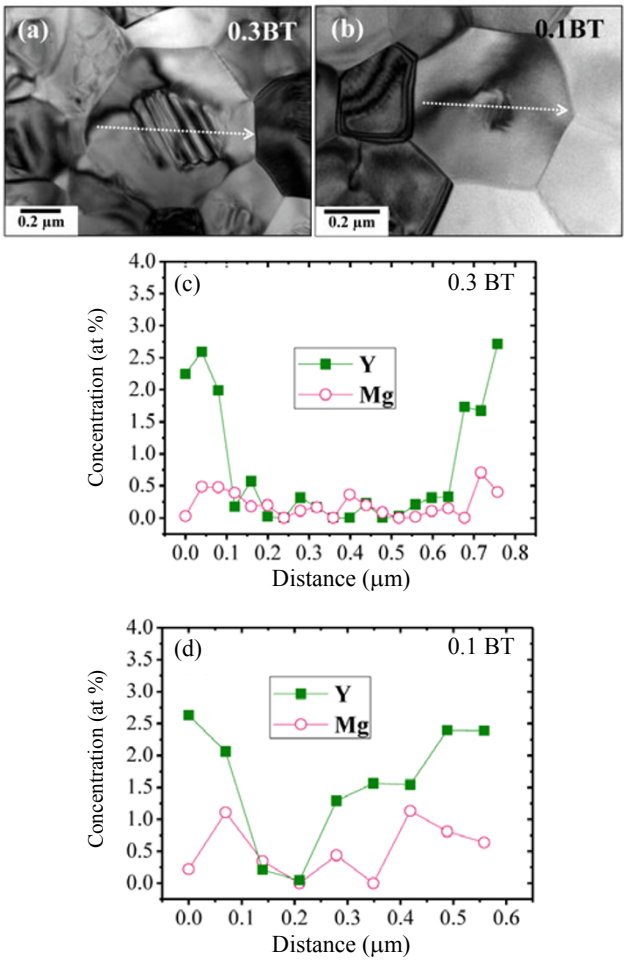

Fig. 3 TEM micrographs and TEM/EDS line scanning results of grains in 0.3BT sample ((a) and (c), respectively) and 0.1BT sample ((b) and (d), respectively).

Figure 4 plots the measured temperature dependence of the dielectric permittivity, the dissipation factor and the temperature coefficient of capacitance (TCC) of the samples in the first set. There are two notable features in Fig. 4. First, as the shell fraction increases under a constant core/shell grain size, the dielectric permittivity decreases remarkably in the high-temperature region (near T_C) while it increases in the low-temperature region (below room temperature). As a result, the TCC curve rotates clockwise with increasing volume fraction of the shell (decreasing core size), as shown in Fig. 4(b). The clockwise rotation of the TCC curve with increasing volume fraction of the shell is attributed to an increased shell contribution. In the case of 0.1BT which has the highest shell fraction, the worst dielectric permittivity temperature stability is observed, as seen in Fig. 4(b). As the growth of core/shell grains is a result of a conversion process from both the core and shell into another shell, the broadening and subsiding of the Curie peak also indicate a decreasing contribution of the ferroelectric core to the overall dielectric properties. In particular, for the 0.1BT sample, the Curie peak vanishes. The disappearance of the Curie peak in 0.1BT might be related to the small core size, although

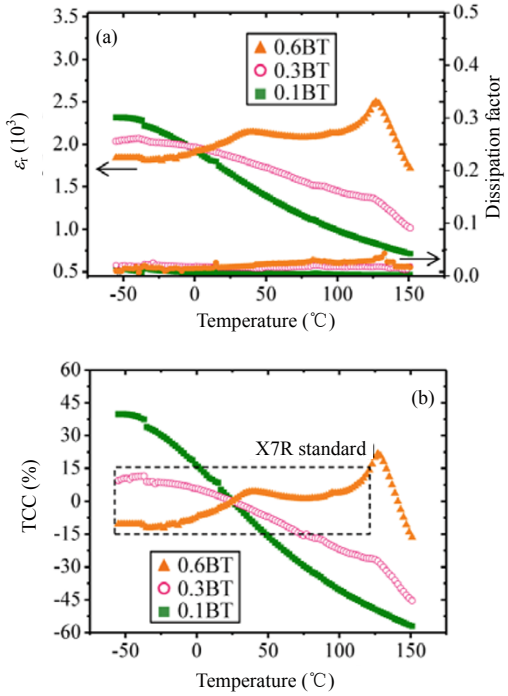

Fig. 4 (a) Measured dielectric properties and (b) TCC curves of the first set for a temperature range of –55–150 ℃.

ferroelectric domains are still present in the cores. It is well documented in the literature that the tetragonality of $BaTiO_3$ gradually decreases as the particle size decreases in a submicron range, and is even lost and becomes cubic (c/a = 1) below a critical particle size (below ~0.1 μm) [28].

Second, the maximum temperature (T_m) at which the maximum dielectric permittivity appears to be shifted towards low temperature with shell thickening. In the shell phase, there should be numerous phase transition temperatures distributed over a wide temperature range depending on the local chemical composition. T_m would then be determined by the T_m value of the chemical composition with the largest volume fraction. The Y concentration in the shell is measured for six core/shell grains and its representative variation with the distance from a core is plotted in Fig. 5. The figure shows that the Y concentration increases as the distance from the core increases. As the volume fraction of a shell with a constant thickness increases with increasing the distance from the center of a grain, the phase with the largest volume fraction in the sample in Fig. 5 is that having the highest Y concentration. According to previous investigations [10,27], T_m decreases with increased Y doping. A reduction of T_m with shell thickening, which is shown in Fig. 4(a), is thus attributed to the increased volumetric layer of a high Y concentration.

Figure 6 shows the microstructural variation in the second set with different sintering time: 0.5 h (denoted as BT-0.5), 1 h (BT-1) and 4 h (BT-4), respectively. From the SEM micrographs, the average 2-dimensional grain sizes are measured to be 0.79 μm for BT-0.5, 0.97 μm for BT-1 and 1.09 μm for BT-4. Figure 6(d) plots the variations of the measured core size and estimated core volumetric percentage with

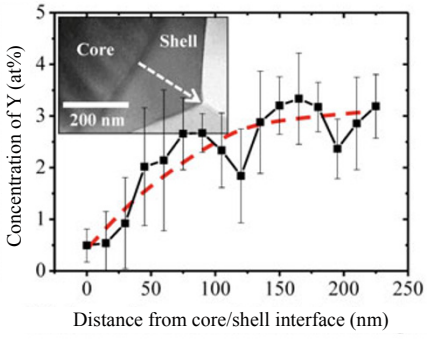

Fig. 5 TEM/EDS result showing the Y concentration in the shell of a grain. The scale bar for each data point represents the standard deviation of five measurements.

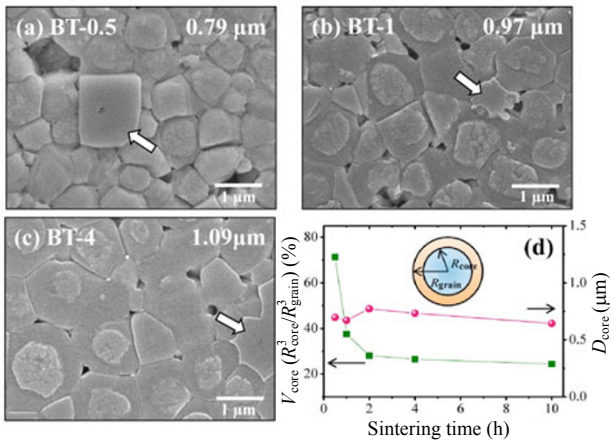

Fig. 6 SEM micrographs of (a) BT-0.5, (b) BT-1 and (c) BT-4 in the second set. (d) Measured core volumetric percentage and core size with respect to sintering time. The numbers in micrographs are the measured average grain sizes.

sintering time. The volumetric percentage of core decreases drastically from 70% after 0.5 h sintering to 24% after 10 h sintering. Meanwhile, the core size remains almost identical at ~0.7 μm.

The observed grain growth must occur via dissolution of $BaTiO_3$ and precipitation of dissolved $BaTiO_3$ together with yttrium through a Y-rich liquid phase, which is present at grain boundaries and triple junctions in all the samples, as indicated by arrows in Fig. 6. The presence of a liquid phase in which $BaTiO_3$ has a sufficient solubility was previously suggested to be a necessary condition for core/shell formation in $BaTiO_3$-based materials [5].

Figure 7 plots the measured temperature dependence of the dielectric permittivity, the dissipation factor and the TCC of the samples in the second set. All of the core/shell samples exhibit stable temperature dependence with low dissipation factors (below 0.03). As the shell fraction increases for the same core size, the dielectric permittivity decreases at high temperature and increases at low temperature (Fig. 7(a)). As a result, the TCC curve rotates clockwise with shell thickening, as shown in Fig. 7(b). Only the BT-0.5 and BT-1 samples with low shell fractions meet the X7R standard. The dielectric-temperature behavior in the second set, however, varies less remarkably than that of the first set. This result may be due to a constant doping amount, irrespective of the shell thickness, as well as to a less significant reduction of the volumetric ratio of the core, from 43.8% for 0.6BT to 3.7% for 0.1BT in the first set and from 71.2% for BT-0.5 to

26.5% for BT-4 in the second set. It is noteworthy that for the studied range, the BT-1 sample with a core volume fraction of ~38% exhibits the best temperature stability with a good dielectric constant. This suggests that for a given dopant amount, there exists an optimum layer thickness for good temperature stability of MLCCs. In our system, a shell thickness of about one third of the core radius appears to be an optimum thickness.

In previous investigations, the effects of the volumetric ratio of core/shell on dielectric-temperature behavior have been studied for samples with different ball milling time [6,25,26], thermal cycle [10] and sintering atmosphere [27]. It was reported that the temperature stability is improved with a reduction of shell thickness. In those previous studies, however, additional effects due to factors such as different chemistry in the shell [10,26,27] and difference in grain size [25,27] might have influenced the results. In addition, the variation of the core/shell fraction is estimated mostly by indirect methods, such as EDS [10,26,27] and synchrotron X-ray diffraction [25].

In the present study, through systematic model experiments with direct microstructural characterization as well as minimized chemical and microstructural effects, it is possible to clarify the effects of the core/shell volumetric ratio on the dielectric-temperature behavior of $BaTiO_3$. For the studied range, it is shown that the shell thickness should be thin in core/shell grains, irrespective of core and grain sizes, to ensure high temperature stability of the dielectric properties. Reduced shell thickness may also contribute to enhanced temperature stability by increasing the probability of maintaining coherency at the interface between the core and the shell, as shown in a recent study [29]. There exists, however, an optimum thickness for a given system. In our study, it is approximately one third of the core radius.

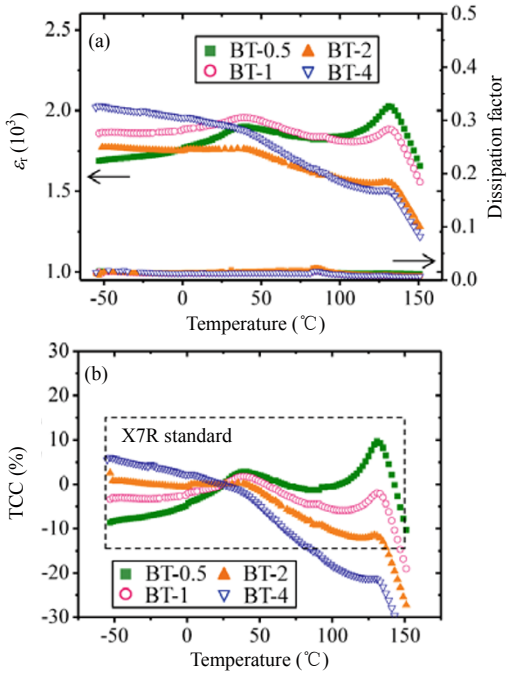

Fig. 7 (a) Measured dielectric properties and (b) TCC curves of the second set for a temperature range of −55–150 ℃.

4 Conclusions

We studied the effects of the relative sizes of cores and shells on the dielectric-temperature behavior of (Mg,Y)-doped $BaTiO_3$ samples. Taking into consideration the dissolution/precipitation mechanism of the shell formation, two different sets of samples with controlled core and grain sizes were prepared by varying the sintering time and the size of the starting $BaTiO_3$ powders. It was shown that the shell needed to be thin enough to improve the temperature stability of the dielectric properties of core/shell grained $BaTiO_3$. For the studied system, shell thickness of about one third of the core radius provided optimum temperature stability. As the shell thickening occurred via a dissolution/precipitation process, control of grain growth was essential to fabricate core/shell grained $BaTiO_3$ with improved dielectric-temperature behavior.

Acknowledgements

This work was supported by the Samsung Electro-Mechanics Co. Ltd. through the Center for Advanced MLCC-Manufacturing Processes and also by the Priority Research Centers Program (Grant No. 2012-048034) through the National Research Foundation of Korea (NRF) funded by the Ministry of Education, Science and Technology (MEST), Korea.

References

[1] Kahn M. Effects of sintering and grain growth on the distribution of niobium addtion in barium titanate ceramics. Ph.D. thesis. University Park (USA): Pennsylvania State University, 1969.

[2] Hennings D, Rosenstein G. Temperature-stable dielectrics based on chemically inhomogeneous $BaTiO_3$. *J Am Ceram Soc* 1984, **67**: 249–254.

[3] Armstrong TR, Young KA, Buchanan RC. Dielectric properties of fluxed barium titanate ceramics with zirconia additions. *J Am Ceram Soc* 1990, **73**: 700–706.

[4] Lu H-Y, Bow J-S, Deng W-H. Core-shell structures in ZrO_2-modified $BaTiO_3$ ceramic. *J Am Ceram Soc* 1990, **73**: 3562–3568.

[5] Randall CA, Wang SF, Laubscher D, *et al*. Structure property relationships in core-shell $BaTiO_3$–LiF ceramics. *J Mater Res* 1993, **8**: 871–879.

[6] Kim C-H, Park K-J, Yoon Y-J, *et al*. Formation of core-shell structure in $BaTiO_3$ grains. *J Korean Ceram Soc* 2009, **46**: 123–130.

[7] Jeon S-C, Lee C-S, Kang S-JL. The mechanism of core/shell structure formation during sintering of $BaTiO_3$-based ceramics. *J Am Ceram Soc* 2012, **95**: 2435–2438.

[8] Chazono H, Kishi H. Sintering characteristics in $BaTiO_3$–Nb_2O_5–Co_3O_4 ternary system: I, Electrical properties and microstructure. *J Am Ceram Soc* 1999, **82**: 2689–2697.

[9] Chou C-C, Chen C-S, Lin I-N, *et al*. Development of X7R type base-metal-electroded $BaTiO_3$ capacitor materials by co-doping of MgO/Y_2O_3 additives. *Ferroelectrics* 2006, **332**: 35–39.

[10] Tian Z, Wang X, Gong H, *et al*. Core-shell structure in nanocrystalline modified $BaTiO_3$ dielectric ceramics prepared by different sintering methods. *J Am Ceram Soc* 2011, **94**: 973–977.

[11] Smolenskii GA. Physical phenomena in ferroelectrics with diffused phase transition. *J Phys Soc Jpn* 1970, **28**: 26–37.

[12] Cross LE. Relaxor ferroelectrics. *Ferroelectrics* 1987, **76**: 241–267.

[13] Kumar MM, Srinivas K, Suryanarayana SV. Relaxor behavior in $BaTiO_3$. *Appl Phys Lett* 2000, **76**: 1330.

[14] Cui L, Hou Y-D, Wang S, *et al*. Relaxor behavior of $(Ba,Bi)(Ti,Al)O_3$ ferroelectric ceramic. *J Appl Phys* 2010, **107**: 054105.

[15] Armstrong TR, Morgens LE, Maurice AK, *et al*. Effects of zirconia on microstructure and dielectric properties of barium titanate ceramics. *J Am Ceram Soc* 1989, **72**: 605–611.

[16] Chazono H, Fujimoto M. Sintering characteristics and formation mechanisms of "core-shell" structure in $BaTiO_3$–Nb_2O_5–Co_3O_5 ternary system. *Jpn J Appl Phys* 1995, **34**: 5354–5359.

[17] Kishi H, Okino Y, Honda M, *et al*. The effect of MgO and rare-earth oxide on formation behavior of core-shell structure in $BaTiO_3$. *Jpn J Appl Phys* 1997, **36**: 5954–5957.

[18] Kim J-S, Kang S-JL. Formation of core-shell structure in the $BaTiO_3$–$SrTiO_3$ system. *J Am Ceram Soc* 1999, **82**: 1085–1088.

[19] Kishi H, Kohzu N, Ozaki N, *et al*. Effect of occupational sites of rare-earth elements on the Curie point in $BaTiO_3$. *Proceedings of the 13th IEEE International Symposium on the Applications of Ferroelectrics* 2002: 271–276.

[20] Nishikawa J, Hagiwara T, Kobayashi K, *et al*. Effects of microstructure on the Curie temperature in $BaTiO_3$–Ho_2O_3–MgO–SiO_2 system. *Jpn J Appl Phys* 2007, **46**: 6999–7004.

[21] Kim CH, Park KJ, Yoon YJ, *et al*. Role of yttrium and magnesium in the formation of core-shell structure of $BaTiO_3$ grains in MLCC. *J Eur Ceram Soc* 2008, **28**: 1213–1219.

[22] Park KJ, Kim CH, Yoon YJ, *et al*. Doping behaviors of dysprosium, yttrium and holmium in $BaTiO_3$ ceramics. *J Eur Ceram Soc* 2009, **29**: 1735–1741.

[23] Kishi H, Kohzu N, Sugino J, *et al*. The effect of rare-earth (La, Sm, Dy, Ho and Er) and Mg on the microstructure in $BaTiO_3$. *J Eur Ceram Soc* 1999, **19**: 1043–1046.

[24] Kishi H, Mizuno Y, Chazono H. Base-metal electrode-multilayer ceramic capacitors: Past, present and future perspectives. *Jpn J Appl Phys* 2003, **42**: 1–15.

[25] Yasukawa K, Nishimura M, Nishihata Y, *et al*. Core-shell structure analysis of $BaTiO_3$ ceramics by synchrotron X-ray diffraction. *J Am Ceram Soc* 2007, **90**: 1107–1111.

[26] Wang T, Wang X, Wen H, *et al*. Effect of milling process on the core-shell structures and dielectric properties of fine-grained $BaTiO_3$-based X7R ceramic materials. *Int J Min Met Mater* 2009, **16**: 345–348.

[27] McCauley DE, Chu MSH, Megherhi MH. PO_2 dependence of the diffuse-phase transition in base metal capacitor dielectrics. *J Am Ceram Soc* 2006, **89**: 193–201.

[28] Yoon D-H. Tetragonality of barium titanate powder for a ceramic capacitor application. *J Ceram Process Res* 2006, **7**: 343–354.

[29] Jeon SC, Kang S-JL. Coherency strain enhanced dielectric-temperature property of rare-earth doped $BaTiO_3$. *Appl Phys Lett* 2013, **102**: 112915.